Poroelastic effects of the damaged zone on fracture reflectivity

Edith Sotelo, Santiago G. Solazzi, J. Germán Rubino, Nicolás D. Barbosa, Klaus Holliger

UNIL | Université de Lausanne
Institut des sciences de la Terre

CONICET

UNIVERSITÉ DE GENÈVE

Motivation

Studies show evidence of a damaged zone surrounding fractures and faults.

Figure 1. Macrofracture density versus distance from fault core. Modified from Mitchell and Faulkner (2009).

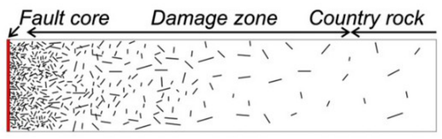

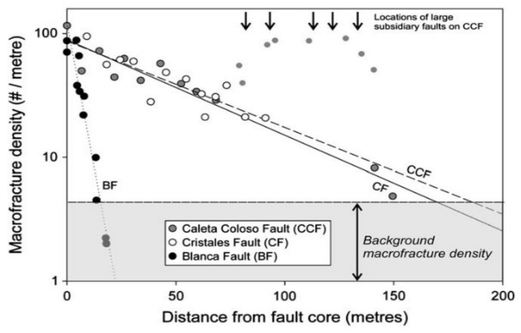

Enhanced permeability associated with damaged zones, in an otherwise largely impermeable background rock, can promote fluid pressure diffusion (FPD) from fractures as seismic waves travel through the system. This process is expected to increase normal compliance of fractures and, in turn, raise their seismic reflectivity.

We calculate reflectivity of a normally-incident P-wave for layered elastic-poroelastic models. In these models, we represent the fracture and associated damaged zone as poroelastic layers. We also consider a model in which the fracture and associated damaged zone are represented by an equivalent viscoelastic (EVE) layer. This representation facilitates the incorporation of complex damaged zone models, e.g. containing discrete fractures. We also calculate normal compliance of the fracture for each model.

Methodology

a) Elastic model **b)** Elastic-poroelastic model **c)** Elastic-viscoelastic model

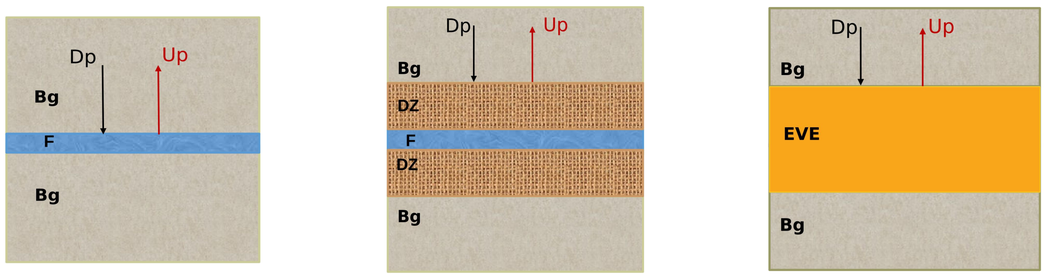

Figure 2. (a) Reference model, (b) model with damaged zones and (c) model with upscaled fracture and associated damaged zones represented by an EVE layer. Bg is the elastic background rock, DZ is the damaged zone and F is the fracture. For model (b), DZ and F are poroelastic layers. Dp and Up are the normally-incident and the reflected P-waves, respectively.

We compute the reflection coefficients at the F-Bg interface (Figure 2a), the DZ-Bg interface (Figure 2b) and Bg-EVE interface (Figure 2c), respectively. To find the corresponding seismic amplitudes, we formulate a system of equations by:

- Imposing continuity of traction, pressure, and solid and relative fluid displacements at the poroelastic interfaces (Biot, 1962; Barbosa et al., 2016).
- Imposing continuity of traction and solid displacement with zero relative fluid displacement at the elastic-poroelastic interfaces.
- Imposing continuity of traction and displacement at the elastic interfaces and elastic-viscoelastic interfaces.

To obtain the EVE layer (Figure 2c), we perform an uspcaling of the poroelastic fracture and associated damaged zones following the analytical technique proposed by White et al. (1975).

Moreover, we calculate normal compliance for the elastic and poroelastic fractures by taking the displacement jump over the average traction at the boundaries of the fracture layer (Schoenberg, 1980). We also calculate normal fracture compliance for the viscoelastic upscaled model following the extension to the aforementioned Schoenberg's defintion as proposed by Rubino et al. (2015).

Results

Table 1. Reference values of rock and fluid properties of the poroelastic thin layer representing the fracture and the associated DZ layers. For the elastic background and fracture we use the fluid and drained rock properties of the DZ and poroelastic fracture, respectively. We also use Gassmann's equations to obtain other elastic properties.

Property	DZ	Fracture
Grain bulk modulus K_s (GPa)	37	37
Grain density ρ_s (Kg/m^3)	2730	2730
Porosity ϕ	0.015	0.8
Frame bulk modulus K_m (GPa)	33	0.004
Frame shear modulus μ (GPa)	29	0.002
Thickness h (m)	0.2	0.001
Permeability κ (D)	0.1	100
Tortuosity S	3	8
Fluid density ρ_f (Kg/m^3)	1000	1000
Fluid bulk modulus K_f (GPa)	2.25	2.25
Fluid viscosity η $(Pa.s)$	0.001	0.001

Figure 3 shows that, compared to the elastic model, there is an increase of reflectivity for the elastic-poroelastic models of approximately one-order magnitude as a consequence of FPD. FPD allows fluid pressure release from the fracture as the pressure equalizes. This, in turn, increases normal fracture compliance (Figure 5) and raises the reflectivity of the system. Observe that, for the given thickness of 0.2 m, there is an upper limit for $|R_{PP}|$ regardless of the permeability κ_r. This happens because the DZ thickness provides a limited pore volume for FPD to occur in its relaxed state. Please note that the permeability κ_r controls the transition frequency f_{dm}, at which reflectivity decreases towards its undrained values.

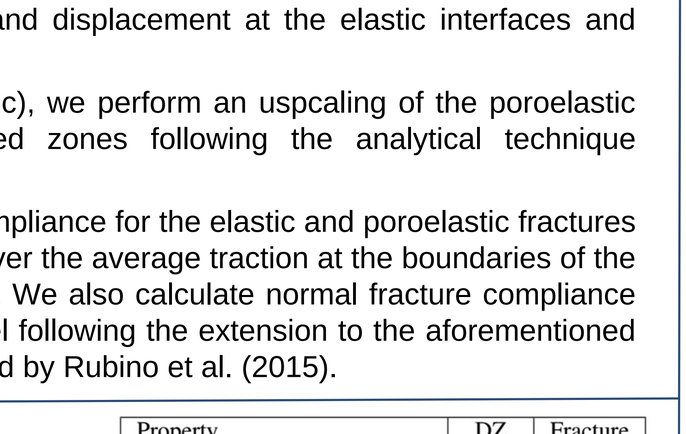

Figure 3. Absolute value of reflectivity $|R_{PP}|$ for a normally-incident P-wave as a function of frequency for different DZ permeabilities κ_r.

Figure 4. Absolute value of reflectivity $|R_{PP}|$ for a normally-incident P-wave as a function of frequency for different DZ thicknesses h_r.

Figure 4 shows that reflectivity increases with h_r. This occurs because a larger DZ thickness provides more pore volume for FPD to happen in its relaxed regime. On the other hand, an increase in DZ thickness shifts the characteristic transition frequency f_{dm} towards lower values.

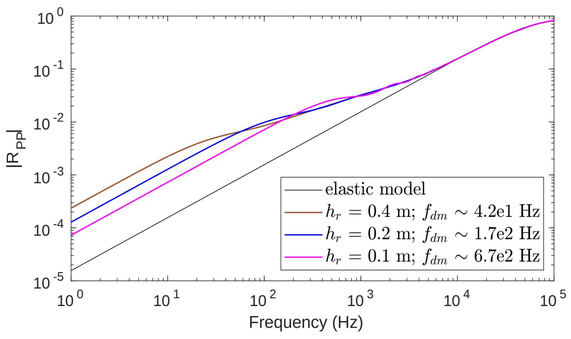

Figure 5. (a) Real and (b) imaginary parts of normal fracture compliance Z_N as a function of frequency for different DZ permeabilities κ_r.

Figure 5 shows that, as expected, the elastic normal compliance is constant for all frequencies. In contrast, the poroelastic normal compliance values become complex and frequency-dependent as the FPD regime transitions from the relaxed to the unrelaxed state. Notice that for sufficiently low frequencies, normal compliance is highest since the fracture experiences the maximum deformation while the maximum fluid exchange occurs between the DZ and the fracture. Note that there is an upper limit value regardless of the DZ permeability, which is constrained by the DZ thickness. This is because thickness limits the pore volume available for FPD. Please note that the DZ permeability controls the transition frequency towards the undrained normal compliance.

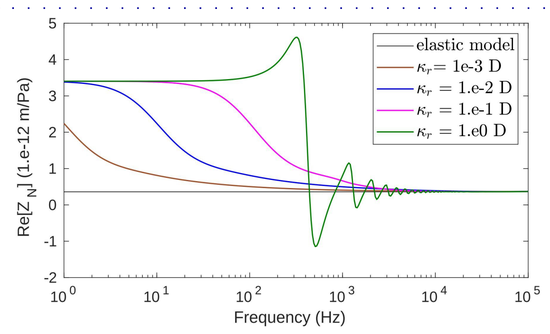

(a)

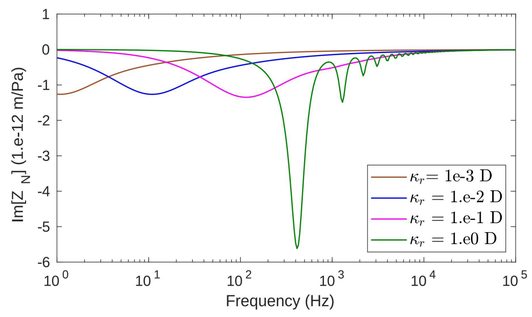

(b)

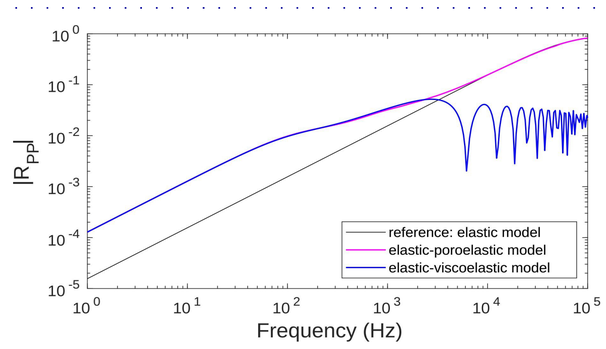

(a)

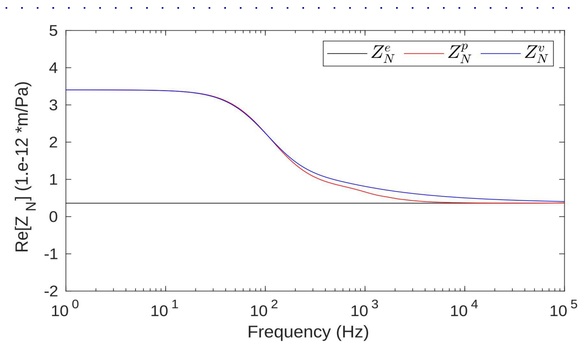

(b)

Figure 6. (a) Absolute value of reflectivity $|R_{PP}|$ and (b) real part of normal fracture compliance Z_N as a function of frequency for the various models. Superscripts e, p and v denote elastic, poroelastic and viscoelastic media, respectively. Values of rock and fluid properties are taken from Table 1.

Figure 6 shows that the upscaled elastic-viscoleastic model reproduces fairly well the reflectivity and normal compliance values of the elastic-poroelastic model up to its first resonance frequency (~ 5250 Hz). The latter results from the scattering created due to the thickness of the equivalent viscoelastic layer (Figure 2c). This viscoelastic upscaling reproduces the mechanical behavior of the set comprised by the poroelastic fracture and the two associated poroelastic DZ layers. In general, the upscaled parameters are frequency-dependent moduli. For this particular 1D case, we obtain the frequency-dependent plane-wave modulus. This upscaling procedure is useful for including complex DZ representatios, e.g including fractures, for which numerical upscaling methods can be applied.

Conclusions

Our results show that FPD between a fracture and its adjacent DZ increases fracture normal compliance as FPD allows fluid pressure release from the fracture into the DZ. As a consequence, the reflectivity of the system also increases when compared to an impermeable reference model. Furthermore, our results also show that the values of the normal compliance and reflectivity are controlled by the DZ thickness and permeability.

On the other hand, the viscoelastic upscaling of the set comprised by the poroelastic fracture and the two associated poroelastic DZ layers reproduces the mechanical response of this poroelastic set. This, in turn, would facilitate the incorporation of more complex DZ representations.

Overall, this study shows that FPD effects promoted by the presence of a DZ in an otherwise impermeable rock can enhance the reflectivity of a fracture in the seismic frequency band.

Acknowledgements

This work is supported by a grant from the National Science Foundation and has been completed within the Swiss Competence Center on Energy Research – Supply of Electricity, with the support of Innosuisse. J. G. R. gratefully acknowledges the financial support received from the Agencia Nacional de Promoción Científica y Tecnológica of Argentina (PICT 2017-2976)

Reference

Barbosa, Nicolás D., et al. (2016) “Fluid pressure diffusion effects on the seismic reflectivity of a single fracture.” The Journal of the Acoustical Society of America 140(4), 2554-2570.

Biot, M. A. (1962). “Mechanics of deformation and acoustic propagation in porous media.” Journal Applied Physics 33, 1482–1498.

Mitchell, T. M., and D. R. Faulkner (2009). “The nature and origin of off-fault damage surrounding strike-slip fault zones with a wide range of displacements: A field study from the Atacama fault system, northern Chile.” Journal of Structural Geology 31(8), 802-816.

Rubino, J. G., Castromán, G. A., Müller, T. M., Monachesi, L. B., Zyserman, F. I., & Holliger, K. (2015). Including poroelastic effects in the linear slip theory. Geophysics, 80(2), A51–A56.

Schoenberg, M. (1980). Elastic wave behavior across linear slip interfaces. The Journal of the Acoustical Society of America, 68(5), 1516–1521.

White, J. E., Mihailova, N., & Lyakhovitsky, F. (1975). Low-frequency seismic waves in fluid-saturated layered rocks. The Journal of the Acoustical Society of America, 57(S1), S30–S30.